78-675

Behavior of Partially Metallized Kapton for Spacecraft Charging Control

Paul A. Robinson Jr.*
Hughes Research Laboratories, Malibu, Calif.

Results of electron beam charging of pure Kapton and mesh-covered Kapton used to control charge buildup on spacecraft are presented. The electron beam energy was varied from 200 eV to over 10,000 eV. The sample with the aluminum grid had about 10% of its total exposed surface area covered with a hexagonal-shaped aluminum grid. The addition of the aluminum grid limits the area involved in arcing. It is able to bleed off some, but not all, of the deposited charge. Experimental data are presented, and a qualitative explanation is suggested.

Introduction

CONTROLLING charge on the dielectric surfaces of a spacecraft is important in preventing electronic malfunctions.[1] When dielectrics cover areas near instruments that are monitoring the environment, charge control is even more important. A charged surface will increase or decrease charged particle fluxes to the instrument. The interpretation of experimental results is severely affected by uncontrolled nearby charged surfaces. One common approach to charge control is to apply conductive paths on the outer surface of the dielectric material and ground the conductor to the spacecraft (see Fig. 1).[2] In that use, charge control was important to the operation of the instruments making plasma measurements and to the spacecraft. The study reported on here explored such a scheme. For comparison, the same material without the conductive grid was also tested. These tests show substantial improvement in dielectric response for the sample with the conductive mesh. The experiments also lend support to the idea of trapped charge within the dielectric dominating material behavior, especially when the samples are exposed to electrons over 15 kV.[3]

Experimental Configuration

Figure 2 is a schematic of the electron gun and sample holder configuration. Five samples are mounted on a wheel, and the wheel is surrounded by a metal shield. The sample of interest is then rotated into position behind a hole cut in the front of the shield. This hole acts as a collimator for the electron beam and leaves at least a 1-cm-wide ring on the outer edge of the sample out of the line of sight of the electron source. Each sample is supported by a 10-cm-diameter stainless-steel plate. During exposure of a sample, the current to the stainless-steel plate on which it is mounted is measured. This is called the "back current." The front surface of the sample is 72.5 cm from the electron source. The total apparatus length is 107 cm. The collimator is 8 cm in diameter and 7 cm in front of the target.

The electron gun is designed to give a wide-angle electron beam. The electron source is a heated tungsten filament. In our implementation of the design, photons from the filament are not allowed to directly illuminate the target. Figure 3 shows the electron gun.[4] Bias voltages to extract the electrons from the region of the filament are applied to the inner electrodes. Most of the acceleration is provided by the final electrode. The electron source is biased negatively so that the electrons, once they leave the gun, are in the field-free region. The target is also initially at ground potential. Voltage measurements are made by positioning a Monroe electrostatic voltmeter with a gradient adaptor in front of the sample. A shield prevents any electrons from the beam from hitting the sample during voltage measurements. The pressure during these tests is kept at 3×10^{-6} Torr or less. The target samples are surrounded by a grounded stainless-steel enclosure. No light is allowed to hit the target.

The experimental setup was checked by measuring the secondary electron emission characteristics of oxygen-free copper. The back current as a function of beam voltage is the same shape as the secondary emission curve for conductors. The results are shown in Fig. 4. They exhibit two zero-current points, V_I at 200 V and V_{II} at 1500 V. There is a broad peak centered about 600 V. These results are in excellent agreement with published results for copper.[5]

The dielectric samples were tested in a similar manner but produced totally different results. These experiments can be divided into three classes: dielectric charge-up, charge redistribution, and arcing or discharging. The charge-up of

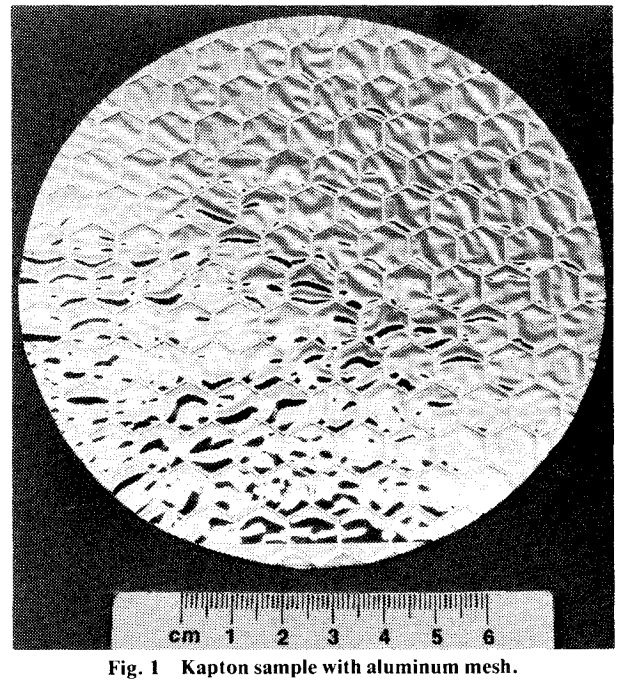

Fig. 1 Kapton sample with aluminum mesh.

Presented as Paper 78-675 at the AIAA/DGLR 13th International Electric Propulsion Conference, San Diego, Calif., April 25-27, 1978; submitted June 22, 1978; revision received Oct. 16, 1978.

Index category: Materials, Properties of.

*Staff Physicist.

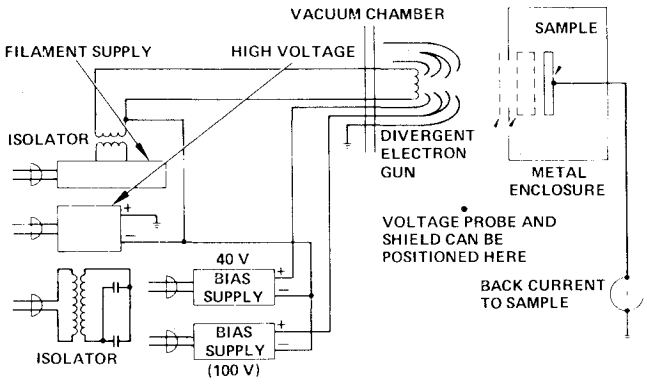

Fig. 2 Schematic representation of experimental apparatus.

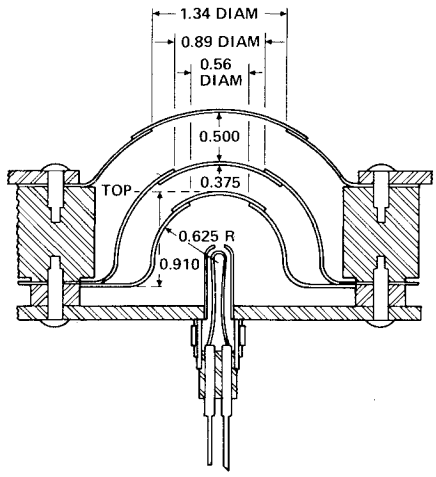

Fig. 3 Divergent electron beam gun (from Ref. 4).

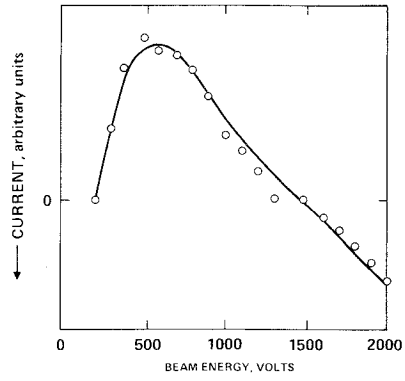

Fig. 4 Secondary emission curve for copper.

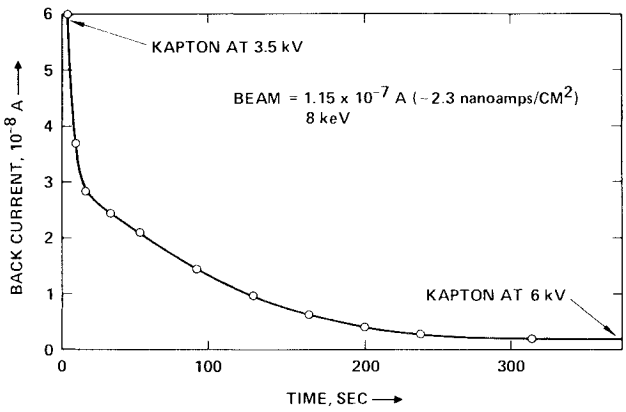

Fig. 5 Typical Kapton charging current vs time.

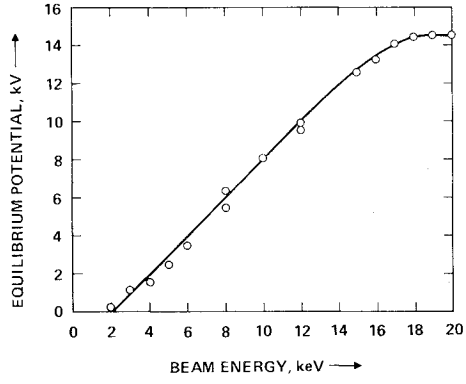

Fig. 6 Equilibrium potential as a function of electron beam energy for Kapton sample.

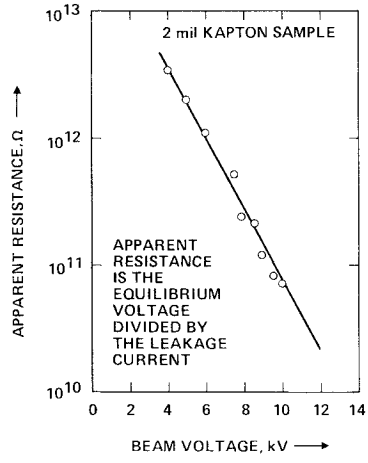

Fig. 7 Apparent resistance versus beam voltage.

the dielectric occurs when the potential on the dielectric changes until it is in equilibrium with the electron beam. The behavior of the dielectric when the electron beam is interrupted by the voltage probe apparatus is an example of charge redistribution. Arcing is the sudden removal of charge from the dielectric. Of primary interest in these tests was a comparison of the gross effects produced by the conductive grid on the dielectric. Of secondary interest was the effect of the grid on the charge transport within the dielectric. This secondary interest led to experiments in which the electron beam was suddenly interrupted. The hope was that this sudden change in the boundary conditions on the front surface of the dielectric would cause a redistribution of trapped charge within the dielectric that could be observed and understood in terms of trapping levels, radiation-induced conductivity, and penetration depths for the dielectric. Unfortunately, reproducible results that can be interrupted in this way have not be obtained. The back currents expected are very small and are easily masked by small electron or ion currents from other sources.

Experiments on dielectric charging can be interpreted in terms of the analysis of Purvis et al.[6] They state that the voltage buildup is governed by

$$V = \frac{1}{C} \int i dt$$

where V is the voltage on the sample, C is the current to the sample, and t is time. The current to the sample can be expressed in terms of the leakage current $i_l = V/R$, the current

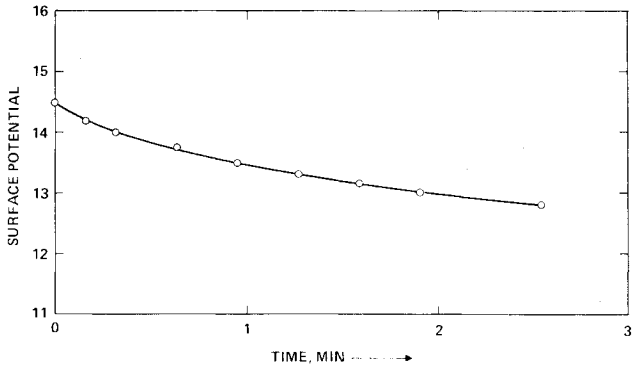

Fig. 8 Decay of voltage with time of Kapton sample, beam energy = 20 keV.

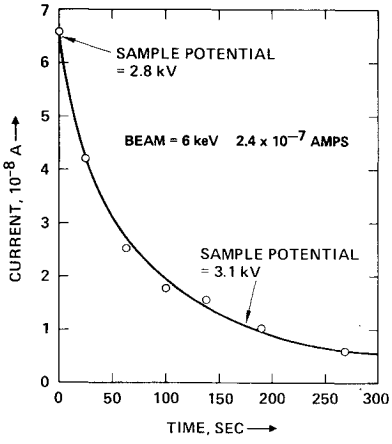

Fig. 9 Mesh design back current.

from the beam $i(V)$, the secondary current i_s, and the backscattered curent i_b. The effects of beam divergence on the total current to the sample are included in $i(V)$. The equilibrium voltage is determined by setting

$$i(V) = i_b + i_s + i_l$$

That is, the net current to the sample is zero. The back current to the sample is

$$i_l + C\frac{dV}{dt}$$

Experimental Results

Two Kapton samples were irradiated in these tests. One was a pure Kapton sample used as a control sample. The second was the mesh design shown in Fig. 1. Both samples were exposed to the electron beam under identical conditions.

Kapton Sample

The Kapton sample is about 12.5 cm in diameter, located behind the 8-cm-diameter collimator. It is 2 mils thick. The back current as a function of time when an 8-keV beam is directed on the Kapton sample is shown in Fig. 5. This is a typical example of back current observed during dielectric charge-up. The results are reproducible. In this case, the initial voltage of the sample was 3.5 kV. At equilibrium, the Kapton sample was at 6 kV. For electron beams with energies below 12 keV, the equilibrium potential of the Kapton sample is roughly 2 kV less than the beam energy. This is shown in Fig. 6. However, above 12 keV the equilibrium potential does not rise as fast as the beam energy and levels off at about 14.5 kV for beam energies above 18 keV. At the same time, the leakage current increases as a function of beam energy. At 20 keV the leakage current accounts for ⅔ of the total beam current. This implies the resistance of the Kapton is decreasing. In Fig. 7 the "apparent resistance," defined as the equilibrium potential divided by the leakage current, is plotted. This effect is reasonable considering the density of electrons above the valence levels in the irradiated region of the Kapton and the high fields. The resistivity calculated from these results is on the order of that measured by Adamo et al.[7] The decrease of resistance at higher beam energies is also seen in the ability of the dielectric to maintain charge when the electron beam is removed. Above 15 keV there is a detectable decay of voltage with time. In Fig. 8 the decay of voltage with time is plotted for a 20-keV electron beam. The initial decay rate is 1 kV/min. At lesser beam voltages the initial voltage rate was less. The initial voltage drop calculated by assuming an exponential decay of resistance with beam voltage is consistent with measured data as shown in Table 1.

Mesh Design Tests

Tests of the mesh design are conducted with the mesh sample replacing the Kapton sample. The aluminum mesh is maintained at ground potential during irradiation. The mesh is 3-mil aluminum that has ben punched in a hexagonal pattern as shown in Fig. 1 and cemented to the Kapton surface.

At low voltages the mesh design behaves very much like the pure Kapton sample. The back current to the mesh design with a beam voltage of 6 keV is shown in Fig. 9. This is typical for charge-up of these samples at beam voltages below 8 kV. At the inception of flashover arcs, when the entire surface participates, a single arc will be followed by a rise in back current and a decay similar to that shown in Figs. 8 and 9. The data in Fig. 10 show the inception of arcing for the grid design. The arcing is not at all regular. The sharp dips, followed by an increase in the magnitude of the current, are believed to be "flashover" arcs in which most of the charge is removed from part of the surface of the dielectric. These current measurements and the fact that no voltages less than 2.3 kV were recorded suggest that only a fraction of the total surface was participating in a flashover at any given time. The spatial resolution of the voltage probe is too large to resolve individual grids; however, the voltage distribution across the sample appears "lumpy," indicating regions of high and low potentials. These regions, which appear to be larger than a single grid pattern, can be interpreted as regions that have recently experienced flashover arcs, as compared to regions which have not. An arc occurred once when the voltage probe was in place, and the measured potential dropped a fraction of the total voltage. This took place when the beam energy was 15 keV. Then the voltage droped from 4 kV to 2.3 kV, and simultaneously a current spike occurred. Typically, a flashover arc would drop the voltage to near zero. The fact that the measured potential was never as high as that measured with the 8-keV beam also suggests that the grid is limiting the spatial extent or arcing.

Figure 11 shows the current to the mesh during irradiation by the 10-keV electron beam. Again, multiple arcs are observed. Our apparatus did not allow simultaneous

Table 1 Voltage decay rate

Beam energy, keV	$\frac{-dV}{dt}$ (calculated), V/min	$\frac{-dV}{dt}$ (measured), V/min
16	260	220
17	390	220
18	550	680
19	770	800
20	1000	950

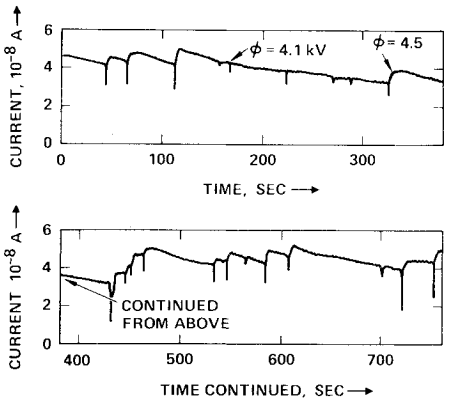

Fig. 10 Back current to mesh design at 10 keV beam energy.

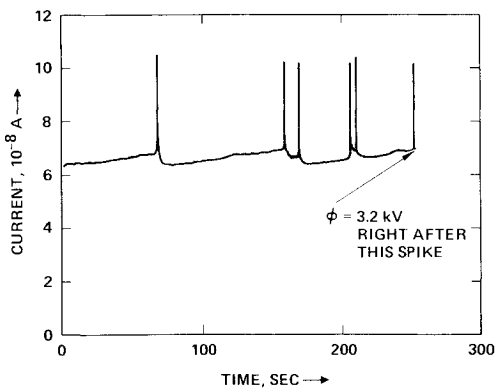

Fig. 11 Current to conductive grid at 10 keV beam energy.

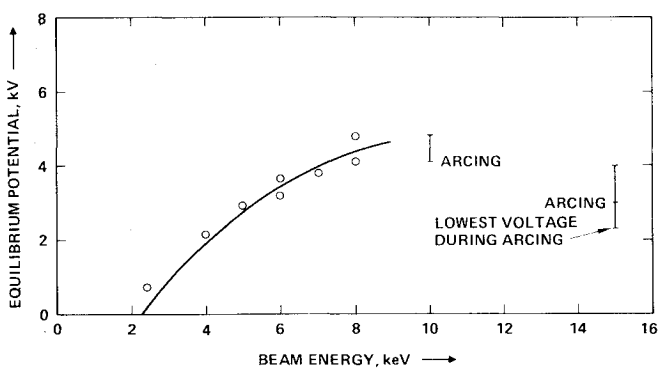

Fig. 12 Equilibrium potential vs beam energy for mesh design.

measurements of both the back current and the current to the mesh, but the current spikes on the mesh must coincide with the current dips of the back current. Results at 15 keV are very similar to those at 10 keV.

Figure 12 summarizes the mesh design's performance as a function of beam energy. Figure 13 compares the mesh design and the Kapton design. At low voltages, the two samples behave similarly, although the mesh design is at a lower

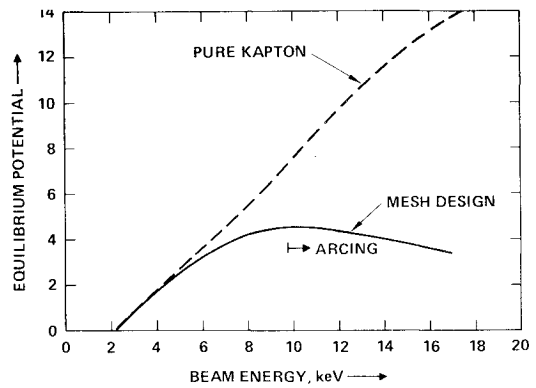

Fig. 13 Comparison of mesh design and Kapton material.

potential than the Kapton. However, above 6 keV the mesh design begins to bleed off charge much more rapidly than does the pure Kapton. Above 10 keV spatially limited arcing is very effective in keeping the average potential below 5 kV with respect to the potential on the mesh.

Conclusions

The addition of a conductive mesh is effective in reducing the equilibrium potential of an otherwise dielectric surface. It is able to do this by both bleeding charges from the beam and dielectric, and by causing arcing in spatially limited areas at lower voltages. At beam energies above 16 keV, the increased conductivity due to electrons implanted in the pure dielectric and/or to the high electric field limits equilibrium potential to about 14.5 kV. The addition of the mesh limits the equilibrium potential to under 5kV.

Acknowledgments

The author gratefully acknowledges the many contributions of C. Dulgeroff and the assistance of J. Mullane and L. Dulmage in completing this study.

References

[1] Pike, C. P. and Lovell, R. R. (eds.), *Proceedings of the Spacecraft Charging Technology Conference,* AFGL-TR77 0051 or NASA TMX 73537, Feb. 1977.

[2] Robinson, P. A., Jr. and Holman, A. B., "Pioneer Venus Spacecraft Charging Model." *Proceedings of the Spacecraft Charging Conference*, Feb. 1977, pp. 298-308.

[3] Meulenberg, A., "Evidence for a New Discharge Mechanism for Dielectrics in a Plasma," *AIAA Proceedings of the American Geophysical Meeting*, June 1975.

[4] "Spacecraft Charging Electron Beam Gun," NASA LeRC Drawing CF635896, Oct. 1975.

[5] Brown, S. C., *Basic Data of Plasma Physics,* MIT Press and Wiley and Sons, 1956.

[6] Purvis, C., K., Stevens, N. J. and Oglebay, J. C., "Charging Characteristics of Materials: Comparison of Experimental Results with Simple Analytical Models," *Proceedings of the Spacecraft Charging Technology Conference*, Feb. 1977, p. 459.

[7] Adamo, R. C., Nanevicz, J. E., and Grier, N., "Conductivity Effects in High Voltage Spacecraft Insulating Materials," *Proceedings of the Spacecraft Charging Technology Conference,* Feb. 1977, p. 669